The Astronomical Journal, 156:194 (10pp), 2018 November https://doi.org/10.3847/1538-3881/aadfe6

Spectroscopic Orbits of Subsystems in Multiple Stars. IV. Double-lined Pairs

Andrei Tokovinin
Cerro Tololo Inter-American Observatory, Casilla 603, La Serena, Chile; atokovinin@ctio.noao.edu
Received 2018 July 18; revised 2018 August 25; accepted 2018 August 29; published 2018 October 12

Abstract

Spectroscopic orbits are computed for inner pairs in nine hierarchical multiple systems (HIP 19639, 60845, 75663, 76816, 78163, 78416, 80448, 84789, and HD 105080) and for one simple binary HIP 61840. All subsystems are double-lined, and their periods range from 2.27 to 30.4 days. Five spectroscopic binaries are twins with equal masses. Each hierarchical system is discussed individually, providing estimates of outer periods, masses, orbital inclination, and axial rotation. For systems with three resolved visual components (HIP 60845 and 80448), the outer and inner visual orbits are determined, complementing the description of their architecture. The radial velocities of HIP 75663A, 76816B, and 78163B are found to be variable with long periods, implying that these hierarchies are 2 + 2 quadruples. The period–eccentricity relation for spectroscopic subsystems is discussed.

Key words: binaries: spectroscopic – binaries: visual

Supporting material: machine-readable tables

1. Introduction

This paper continues the series on spectroscopic orbits of stars belonging to hierarchical systems (Tokovinin 2016a, 2016b, 2018b). It is motivated by the need to improve statistics of orbital elements in stellar hierarchies. Statistics will inform us on the processes of their formation and dynamical evolution, as outlined in the previous papers of this series. This work augments the collection of observational data on stellar hierarchies assembled in the multiple star catalog (MSC; Tokovinin 2018a).

The systems studied here are presented in Table 1. Only one of them (HIP 61840) is a simple binary belonging to the 67 pc sample of solar-type stars; others contain from three to five components and are also relatively close to the Sun. Their principal components are main-sequence stars with spectral types from F2V to G3V. The data in Table 1 are collected from Simbad and *Gaia* DR2 (Gaia Collaboration et al. 2018, in preparation), the radial velocities (RVs) are determined here (variable RVs are marked by "v").

The structure of this paper is similar to the previous ones. The data and methods are briefly recalled in Section 2, where the new orbital elements are also given. Then in Section 3 each system is discussed individually. The paper closes with a short summary in Section 4.

2. Observations and Data Analysis

2.1. Spectroscopic Observations

The spectra used here were taken with the 1.5 m telescope sited at the Cerro Tololo Inter-American Observatory (CTIO) in Chile and operated by the SMARTS Consortium.[1] The observing time was allocated through NOAO. Observations were made with the CHIRON optical echelle spectrograph (Tokovinin et al. 2013) by the telescope operators in service mode. In two runs, 2017 August and 2018 March, the author also observed in classical mode. All spectra are taken in the slicer mode with a resolution of $R = 80{,}000$ and a signal-to-noise ratio of at least 20. Thorium–Argon calibrations were recorded for each target.

Radial velocities are determined from the cross-correlation function (CCF) of echelle orders with the binary mask based on the solar spectrum, as detailed in Tokovinin (2016a). The RVs derived by this method should be on the absolute scale if the wavelength calibration is accurate. The CHIRON RVs were checked against standards from Udry et al. (1998), and a small offset of $+0.15\ \mathrm{km\ s^{-1}}$ was found in Tokovinin (2018b).

The CCF contains two dips in the case of double-lined systems studied here. The dip width is related to the projected rotation speed $V \sin i$, while its area depends on the spectral type, metallicity, and relative flux. Table 2 lists average parameters of the Gaussian curves fitted to the CCF dips. It gives the number of averaged measurements N (blended CCFs were not used), the dip amplitude a, its dispersion σ, the product $a\sigma$ proportional to the dip area (hence to the relative flux), and the projected rotation velocity $V \sin i$, estimated from σ by the approximate formula given in Tokovinin (2016a). The last column indicates the presence or absence of the lithium 6708 Å line in individual components.

2.2. Speckle Interferometry

Information on the resolved subsystems is retrieved from the Washington Double Star Catalog (WDS; Mason et al. 2001). It is complemented by recent speckle interferometry at the Southern Astrophysical Research (SOAR) telescope. The latest publication (Tokovinin et al. 2018) contains references to previous papers.

2.3. Orbit Calculation

As in Paper III (Tokovinin 2018b), orbital elements and their errors are determined by the least-squares fits with weights inversely proportional to the adopted errors. The IDL code `orbit` (Tokovinin 2016c)[2] is used. It can fit spectroscopic, visual, or combined visual/spectroscopic orbits. Formal errors of orbital elements are determined from these fits. The elements

[1] http://www.astro.yale.edu/smarts/

[2] Codebase: http://www.ctio.noao.edu/~atokovin/orbit/ and https://doi.org/10.5281/zenodo.61119.

Table 1
Basic Parameters of Observed Multiple Systems

WDS (J2000)	Comp.	HIP	HD	Spectral Type	V (mag)	$V-K$ (mag)	μ^*_α (mas yr^{-1})	μ_δ	RV (km s^{-1})	$\overline{\omega}$[a] (mas)
04125−3609	A	19639	26758	F3V	7.12	1.12	61	24	35.40	7.94
	B	19646	26773	F2IV	7.91	0.92	61	24	35.98	8.03
12059−4951	A	⋯	105080	G3V	9.13	1.43	25	−15	50.19	9.99
	B	⋯	105081	G0V	9.18	1.42	31	−20	50.09	7.20
12283−6146	A	60845	108500	G3V	6.82	1.64	71	−160	40.02	19.93
	D	⋯	⋯	⋯	13.70	4.54	73	−169	⋯	19.91
12404−4924	A	61840	110143	G0V	7.60	2.00	−28	−112	6.76	18.59
15275−1058	A	75663	137631	G0	8.14	1.35	−65	−35	−56.0 v	9.29
	B	⋯	⋯	G0	9.21	1.50	−61	−35	−56.82	7.69
15410−1449	A	76816	139864	F8V	9.47	1.62	−26	−1	−38.94	3.23
	B	⋯	⋯	⋯	9.74	2.51	−25	−2	−50.9 v	3.15
15577−3915	A	78163	142728	G3V	9.04	1.54	17	6	9.41	10.42
	B	⋯	⋯	⋯	10.30	⋯	31	4	6.78 v	13.57
16005−3605	A	78416	143215	G1V	8.65	1.32	−26	−41	1.60	9.33
	B	⋯	⋯	⋯	9.32	1.31	−28	−41	1.43	9.31
16253−4909	AB	80448	147633	G2V	7.5?	2.3?	−95	−94	−2.08	19.66
17199−1121	A	84789	156769	F2	9.11	1.37	6	13	5.62	5.33
	B	⋯	⋯	⋯	9.89	1.37	5	12	5.97	5.34

Note.
[a] Proper motions and parallaxes are from the *Gaia* DR2 (Gaia Collaboration et al. 2016; Gaia Collaboration et al. 2018, in preparation).
(This table is available in machine-readable form.)

of spectroscopic orbits are given in Table 3 in common notation.

For two multiple systems, the resolved measurements of inner and outer pairs are represented by visual orbits. Simultaneous fitting of inner and outer orbits is done using the code `orbit3.pro` described by Tokovinin & Latham (2017); the code is available in Tokovinin (2017).[3] It accounts for the wobble in the trajectory of the outer pair caused by the subsystem. The wobble amplitude is f times smaller than the inner semimajor axis, where the wobble factor $f = q_{\rm in}/(1+q_{\rm in})$ depends on the inner mass ratio $q_{\rm in}$. The elements of visual orbits are given in Table 4. As outer orbits are poorly constrained, I do not list their errors. The outer orbits serve primarily to model the observed part of the trajectory for the determination of f. In the figures illustrating these orbits, the observed trajectories are plotted relative to the primary component of each system, on the same scale.

Individual RVs of spectroscopic binaries and their residuals to the orbits are presented in Table 5. The HIP or HD number and the system identifier (components joined by a comma) in the first two columns define the binary. Then follow the Julian date, the RV of the primary component V_1, its adopted error σ_1 (blended CCF dips are assigned large errors), and its residual $(O-C)_1$. The last three columns give velocities, errors, and residuals of the secondary component. Table 6 contains RVs of other components, both constant and variable. Finally, Table 7 lists position measurements used for the calculation of visual orbits. It contains the HIP or HD number, system identification, date of observation, position angle θ, separation ρ, adopted error σ_ρ (errors in radial and tangential directions are considered to be equal), and the residuals to the orbits in θ and ρ. The last column indicates the measurement technique. Measurements of the outer systems are of two kinds: when the inner pair is unresolved (e.g., HIP 60845 A,BC), they refer to the photo-center of the inner pair, while resolved measurements refer to the individual components (e.g., HIP 60845 A,B). The orbit-fitting code accounts for reduced wobble amplitude of unresolved (photo-center) measurements compared to resolved ones.

[3] Codebase: https://doi.org/10.5281/zenodo.321854.

3. Individual Objects

For each observed system, the corresponding figure shows a typical double-lined CCF (the Julian date and components' designations are marked on the plot) together with the RV curve representing the orbit. In the RV curves, squares denote the primary component, triangles denote the secondary component, while the full and dashed lines plot the orbit.

3.1. HIP 19639 and 19646 (Triple)

The 50″ pair of bright stars HIP 19639 and 19646 was identified as a visual binary by J. F. W. Hershel in 1838. The *Gaia* DR2 astrometry leaves no doubt that this pair is physical: the components have common proper motion (PM), distance, and RV. The outer orbital period is of the order of 240 kyr. Nordström et al. (2004) found that the component A is a double-lined binary; its 2.35 day circular orbit is determined here for the first time (Figure 1). Two spectra (JD 2458052 and 2458053) were taken with the NRES spectrograph, as described in Tokovinin (2018b).

The CCF of the stronger component Aa is wide and asymmetric, while the CCF of Ab is narrower; their widths correspond to approximate projected rotation velocities $V \sin i$ of 21.7 and 8.7 km s^{-1}, respectively, while the ratio of the CCF areas implies $\Delta V_{\rm Aa,Ab} = 1.50$ mag. Wide and shallow dips lead to large RV errors and large residuals to the orbit. The mass ratio in the inner pair is $q_{\rm Aa,Ab} = 0.82$. The RV of the component B its close to the center-of-mass velocity of A. The component B also has a wide CCF corresponding to $V \sin i$ of ∼33 km s^{-1}.

Table 2
CCF Parameters

HIP/HD	Comp.	N	a	σ (km s^{-1})	$a\sigma$ (km s^{-1})	$V \sin i$ (km s^{-1})	Li 6708 Å
HIP 19639	Aa	7	0.061	12.53	0.765	21.7	N
HIP 19639	Ab	7	0.033	5.90	0.193	8.7	N
HIP 19646	B	2	0.042	18.87	0.787	33:	N
HD 105080	A	3	0.389	3.68	1.429	2.5	N
HD 105081	Ba	11	0.179	3.82	0.684	3.1	N
HD 105081	Bb	11	0.167	3.78	0.630	3.0	N
HIP 60845	Aa	2	0.183	3.83	0.702	3.2	N
HIP 60845	Ab	2	0.124	4.01	0.497	3.8	N
HIP 60845	BC	2	0.430	3.57	1.535	2.0	N
HIP 61840	Aa	9	0.189	4.51	0.853	5.3	Y
HIP 61840	Ab	9	0.124	4.13	0.511	4.2	Y
HIP 75663	A	5	0.223	6.85	1.528	10.7	Y
HIP 75663	Ba	12	0.161	4.88	0.789	6.3	Y
HIP 75663	Bb	12	0.155	4.87	0.754	6.3	Y
HIP 76816	Aa	6	0.110	8.14	0.899	13.3	Y
HIP 76816	Ab	6	0.030	4.49	0.137	5.3	Y
HIP 76816	B	5	0.506	3.78	1.913	3.0	Y
HIP 78163	Aa	9	0.197	4.08	0.803	4.0	Y
HIP 78163	Ab	9	0.192	4.05	0.778	4.0	Y
HIP 78163	B	3	0.371	4.67	1.732	5.8	N
HIP 78416	Aa	9	0.047	15.43	0.725	27:	Y
HIP 78416	Ab	9	0.041	13.18	0.536	23:	Y
HIP 78416	B	4	0.058	22.68	1.324	40:	Y
HIP 80448	Aa	2	0.101	12.30	1.247	21.3	Y
HIP 80448	Ab	2	0.023	9.78	0.221	16.5	Y
HIP 80448	B	3	0.171	8.62	1.469	14.3	Y
HIP 84789	Aa	6	0.043	12.41	0.536	21.5	N
HIP 84789	Ab	6	0.048	10.88	0.522	18.6	N
HIP 84789	B	2	0.036	27.49	0.996	49:	N

(This table is available in machine-readable form.)

Components of the triple system HIP 19639 are placed on the color–magnitude diagram (CMD) in Figure 2, using the distance modulus of 5.47 mag. The V magnitudes of Aa and Ab are estimated from the combined magnitude of A and the spectroscopic magnitude difference of 1.5 mag. The $V-K$ color of Ab, not measured directly, is assumed to place it on the main sequence. It is clear that both Aa and B are located above the main sequence, near the turn-off. Their positions match reasonably well with the 2 Gyr isochrone and correspond to the masses of 1.6 and 1.5 $\mathcal{M}_\odot$. The mass of Ab deduced from the isochrone is 1.28 $\mathcal{M}_\odot$, matching the spectroscopic mass ratio, while the radii of Aa and Ab are 2.7 and 1.1 $R_\odot$. The orbital axis $a_1 + a_2 = 10.6\,R_\odot$ means that the binary is detached. However, contact and mass transfer are imminent when Aa expands further.

The spectroscopic mass sum of the inner binary is only 0.18 $\mathcal{M}_\odot$. The mass sum estimated above, 2.88 $\mathcal{M}_\odot$, implies an inclination $i_{\rm Aa,Ab} = 23\overset{\circ}{.}4$, or $\sin i_{\rm Aa,Ab} = 0.40$, hence the synchronous rotation velocities of Aa and Ab are 23.8 and 9.7 km s^{-1}, respectively, in agreement with the measured CCF width. Summarizing, this is an interesting triple system where the inner close binary is caught at evolutionary phase preceding the mass transfer.

3.2. HD 105080 and 105081 (2+2 Quadruple)

Two nearly equal stars HD 105080 and 105081 form a 12.″9 physical binary, first measured by J. Hershel in 1835. Each of these stars is a close pair, making the whole system quadruple. The pair Aa,Ab is a known visual binary RST 4958 with a small magnitude difference. Since its discovery in 1942 by R. A. Rossiter, it was observed only episodically. By adding three speckle measures made at SOAR in 2017 and 2018, a preliminary orbit with $P = 91.6$ years can be fitted to the observations (Table 4). Double lines were reported for this star in the literature, although there could be confusion with the double-lined component B. The RV of A is practically coincident with the center-of-mass velocity of B. The *Gaia* DR2 parallax of A has a large error of 1 mas, being affected by the Aa,Ab pair. I adopt the parallax of B as the distance to the system. Both components are then located on the CMD very close to each other, above the main sequence. This distance and the visual orbit of Aa,Ab correspond to the mass sum of 1.7 $\mathcal{M}_\odot$; however, the orbit is poorly constrained.

The component B (HD 105081), which is only slightly fainter than A in the V and G bands, is revealed here to be a twin double-lined pair with $P = 30.4$ days and eccentricity $e = 0.42$ (Figure 3). The spectroscopic mass sum of Ba and Bb, 1.98 $\mathcal{M}_\odot$, and the mass sum inferred from the absolute magnitudes, 2.26 $\mathcal{M}_\odot$, imply inclination $i_{\rm Ba,Bb} = 73°$. The CCF dips of Ba and Bb are narrow and deep, hence the residuals to the orbit are small, only 0.07 km s^{-1}.

3.3. HIP 60845 (Quintuple)

This multiple system is located within 50 pc from the Sun and contains at least five stars arranged in a rare three-tier hierarchy illustrated in Figure 4. The widest 7.″9 pair

Table 3
Spectroscopic Orbits

HIP/HD	System	P (days)	T (+24,00,000)	e	ω_A (degree)	K_1 (km s^{-1})	K_2 (km s^{-1})	γ (km s^{-1})	rms$_{1,2}$ (km s^{-1})	$M_{1,2}\sin^3 i$ ($\mathcal{M}_\odot$)
HIP 19639	Aa,Ab	2.35254	58002.5732	0.0	0.0	39.474	49.194	35.400	0.36	0.094
		±0.00005	±0.0019	fixed	fixed	±0.160	±0.298	±0.100	0.87	0.076
HD 105081	Ba,Bb	30.427	58214.038	0.418	82.1	46.856	47.493	50.099	0.07	1.00
		±0.006	±0.023	±0.001	±0.3	±0.117	±0.118	±0.041	0.05	0.98
HIP 60845	Aa,Ab	6.3035	58195.6279	0.0	0.0	31.361	32.128	40.018	0.10	0.084
		±0.0001	±0.0017	fixed	fixed	±0.063	±0.114	±0.036	0.27	0.082
HIP 61840	Aa,Ab	9.6717	58194.383	0.007	357.0	56.665	60.744	6.745	0.05	0.84
		±0.0008	±0.345	±0.001	±13.0	±0.525	±0.562	±0.048	0.05	0.78
HIP 75663	Ba,Bb	22.8704	58204.4963	0.613	260.1	49.001	49.622	−56.847	0.29	0.56
		±0.0047	±0.020	±0.001	±0.3	±0.126	±0.134	±0.045	0.27	0.56
HIP 76816	Aa,Ab	6.95176	58197.3528	0.0	0.0	45.790	62.448	−39.145	0.29	0.53
		±0.00002	±0.0063	fixed	fixed	±0.306	±0.570	±0.186	1.13	0.39
HIP 78163	Aa,Ab	21.8186	58202.091	0.577	301.0	45.429	45.671	9.411	0.04	0.47
		±0.0015	±0.014	±0.002	±0.3	±0.161	±0.186	±0.045	0.04	0.46
HIP 78416	Aa,Ab	21.0802	58197.2344	0.708	99.1	64.636	71.737	1.636	0.16	1.03
		±0.0030	±0.0072	±0.003	±0.3	±0.372	±0.509	±0.112	0.61	0.93
HIP 80448	Aa,Ab	2.2699	58195.5948	0.0	0.0	73.124	108.452	−1.848	0.64	0.84
		±0.0002	±0.0033	fixed	fixed	±0.592	±0.698	±0.270	0.51	0.57
HIP 84789	Aa,Ab	2.2758	58196.7968	0.0	0.0	78.044	79.004	5.624	0.40	0.46
		±0.0001	±0.0020	fixed	fixed	±0.181	±0.182	±0.073	0.21	0.45

(This table is available in machine-readable form.)

RST 4499 AB,D is physical, based on its stable relative position and the *Gaia* DR2 parallaxes and PMs of the components. The fast (175 mas yr^{-1}) PM facilitates discrimination between physical and optical companions, despite the high stellar density in this field and the faintness of D ($V = 13.4$ mag). The period of AB,D estimated from its projected separation $\rho_{AB,D} = 7\farcs88$ is about 4 kyr and corresponds to the chracteristic orbital velocity $\mu^* = 2\pi\rho_{AB,D}/P_{AB,D} = 13$ mas yr^{-1}. The relative PM between A and D, measured by *Gaia* and corrected for the orbital motion of A, is 11 mas yr^{-1}; it is directed almost exactly toward A (position angle 240°), as indicated by the arrow in Figure 4. If D moves on an eccentric orbit, it will come close to A,BC in ∼700 years, disrupting the system. Alternatively, the observed motion might correspond to a highly inclined and not very eccentric outer orbit, in which case the system could be dynamically stable. If the pair AB,D is bound, the true separation between A and D cannot exceed its projected separation by more than ∼2 times, given their relative speed of 11 mas yr^{-1} and the total mass sum of 4.5 $\mathcal{M}_\odot$.

The visual binary A,BC (CPO 12), for which a crude orbit with $P = 2520$ years and semimajor axis of $5\farcs4$ has been published by Seymour et al. (2002), occupies the intermediate hierarchical level. This orbit is poorly constrained by the century-long observed arc. I computed an alternative orbit with $P_{A,BC} = 690$ years, with smaller eccentricity and semimajor axis (Table 4). This orbit makes more sense, given the threat to dynamical stability posed by the outer component D. Even then, the period ratio $P_{AB,D}/P_{A,BC} \sim 5$ is comparable to the dynamical stability limit. On the other hand, the nearly circular orbit of the inner pair B,C (RST 4499) with $P = 28.2$ years is definitive. The visual orbits and the estimated mass sums match the *Gaia* DR2 parallax reasonably well. Both orbits are retrograde and have small inclinations.

The visual primary star A was identified as a spectroscopic binary by Nordström et al. (2004). Now its 6.3 day double-lined orbit is determined (Figure 5). The eccentricity does not differ from zero significantly, hence the circular orbit is imposed. The masses of Aa and Ab are almost equal, as are their CCF dips. Given the small angular distance between A and BC, $2\farcs06$, the light is mixed in the fiber, so the CCF often has three dips; the CCF shown in Figure 5 is an exception recorded with good seeing and careful guiding. The magnitude difference between Ab and Aa is 0.37 mag, hence their individual V magnitudes are 7.79 and 8.16 mag. By comparing the mass sum of Aa and Ab estimated from their absolute magnitudes, 2.2 $\mathcal{M}_\odot$, with the spectroscopic mass sum of 0.167 $\mathcal{M}_\odot$, I find that the orbit of Aa,Ab has a small inclination of $i_{Aa,Ab} \approx 25°$. The synchronous rotation of the component Aa, of one solar radius, implies the projected rotation of $V \sin i = 3.3$ km s^{-1}, close to the measured value. The three inner orbits could be close to coplanarity, given their small inclinations.

The CCF dip corresponding to the combined light of BC is narrow and has a constant RV of 42.5 km s^{-1}, close to the center-of-mass velocity of A. Slow axial rotation, location of components on the main sequence in the CMD, and nondetection of the lithium line suggest that this quintuple system is relatively old.

3.4. HIP 61840 (Binary)

Unlike the rest of the objects in this paper, this star is a simple spectroscopic binary without additional components. It belongs to the 67 pc sample of solar-type stars (Tokovinin 2014) and is young, as inferred from the chromoshperic activity, X-ray flux, and the presence of lithium in its atmosphere. The double-lined nature was announced by Wichman et al. (2003) and Nordström et al. (2004), but the orbital period was, so far, unknown. The object has been observed by speckle interferometry at SOAR in 2011 and 2016 and found unresolved.

The orbit with $P = 9.67$ days has a small, but significantly nonzero eccentricity $e = 0.007 \pm 0.001$ (Figure 6). The residuals to the circular orbit are 0.3 km s^{-1}, 6× larger than

Table 4
Visual Orbits

HIP/HD	System	P (years)	T (years)	e	a (arcsec)	Ω_A (degree)	ω_A (degree)	i (degree)
HD 105080	Aa,Ab	91.6	1999.15	0.40	0.176	5.4	224.1	40.4
HIP 60845	A,BC	690	1826.7	0.20	2.485	104.4	156.6	141.4
HIP 60845	B,C	28.2	1990.2	0.166	0.221	162.8	77.3	156.1
		±0.2	±0.3	±0.009	±0.003	±6.5	±5.9	±2.5
HIP 80448	A,B	1950	1926.58	0.63	4.644	75.5	267.9	152.1
HIP 80448	Ba,Bb	20.0	2018.08	0.42	0.176	6.1	150.9	109.1
		±0.3	±0.24	±0.02	±0.003	±1.2	±4.9	±0.8

(This table is available in machine-readable form.)

to the eccentric orbit. The masses of Aa and Ab estimated from absolute magnitudes are 1.24 and 1.13 $\mathcal{M}_\odot$, the spectroscopic mass sum is 1.62 $\mathcal{M}_\odot$, hence the inclination is $i = 62°$. The measured projected rotation speed matches the synchronous speed.

3.5. HIP 75663 (2+2 Quadruple)

This system is quadruple. The outer 9.″4 pair was discovered in 1825 by W. Struve. Its estimated period is 17 kyr. Nordström et al. (2004) noted double lines in the visual secondary B. Its orbital period is 22.9 days (Figure 7), with a large eccentricity of $e = 0.61$ and the mass ratio $q_{\rm Ba,Bb} = 0.997$ (a twin). The areas of the CCF dips of Ba and Bb are equal to within 2%. The masses estimated from absolute magnitudes are 1.02 $\mathcal{M}_\odot$ each, leading to the orbital inclination of $i_{\rm Ba,Bb} = 55°$. The axial rotation of Ba and Bb is faster than synchronous, as expected for such an eccentric orbit.

The RV of the main component A is variable according to the CHIRON data (range from −50.7 to −57.3 km s^{-1}) and the literature. Nordström et al. (2004) made two measurements averaging at −58.2 km s^{-1} and suspected RV variability, while *Gaia* measured −55.4 km s^{-1}. The photo-center motion of A caused by the subsystem Aa,Ab could explain the discrepancy between the *Gaia* DR2 parallaxes of A and B (9.29 ± 0.16 and 7.69 ± 0.07 mas, respectively). A similar discrepancy of parallaxes exists in the HD 105080/81 system, where A is a visual binary. The period of Aa,Ab is not known; presumably it is longer than a year. Isaacson & Fischer (2010) classified this star as chromospherically active and found the RV jitter of 4.2 m s^{-1}. The location of the component A on the CMD indicates that it is slightly evolved and matches approximately the 4 Gyr isochrone. Lithium is detectable in the spectra of A and B.

3.6. HIP 76816 (2+2 Quadruple)

This is a quadruple system located at 309 pc from the Sun. The 5.″4 visual binary HWE 37 has been known since 1876; its estimated period is 33 kyr. Double lines in the component A were discovered by Desidera et al. (2006). I used their measurement to refine the period of the circular orbit of Aa,Ab with $P = 6.95$ days, determined here (Figure 8). The eccentric orbit has similar residuals, hence the circular solution is retained. The components Aa and Ab are unequal in the amplitudes of their CCF dips (area ratio 0.152, or 2.0 mag difference) and of the RV variation (mass ratio 0.735). The RV of the visual component B is also variable with a long, still unknown period. I measured its RV at −50.9 km s^{-1} (constant), while *Gaia* measured −41.4 km s^{-1} and Desidera et al. (2006) measured −37.5 km s^{-1}; these RVs differ from the center-of-mass velocity of A, −39.94 km s^{-1}.

The matching *Gaia* DR2 parallaxes place both A and B above the main sequence. The component B is more evolved: it is brighter than A in the K band (unless its K magnitude measured by 2MASS is distorted by the proximity of A, as happens with other close pairs). The mass sum of Aa and Ab, estimated crudely from the absolute magnitudes, is almost 3 $\mathcal{M}_\odot$, leading to the orbital inclination of 42°.5. The stars Aa and Ab apparently rotate synchronously with the orbit.

3.7. HIP 78163 (2+2 Quadruple)

This multiple system is composed by the outer 7.″9 pair WG 185 (estimated period 8 kyr) and the inner subsystem Aa,Ab discovered by Nordström et al. (2004). For the latter, I determined here the orbit with $P = 21.8$ days (Figure 9), $e = 0.58$, and mass ratio $q_{\rm Aa,Ab} = 0.996$ (a twin). The RV of the component B measured with CHIRON ranges from 6.1 to 7.1 km s^{-1} and differs from the center-of-mass RV of the component A, 9.4 km s^{-1}. Considering also the *Gaia* RV(B) = 16.3 km s^{-1}, I infer that B is a single-lined binary, possibly with a long period and a small RV amplitude. Its photo-center motion could explain the slight discrepancy between *Gaia* parallaxes and PMs of A and B. Therefore, the parallax of A, 10.42 mas, is likely the correct one.

The twin components Aa and Ab have masses of one solar each. Comparing them to $M \sin^3 i$, the inclination of 50° is derived. The stars A and B are located on the main sequence. Interestingly, lithium is detectable in the spectra of Aa and Ab, but not in B, which is a similar solar-mass star.

3.8. HIP 78416 (Triple or Quadruple)

The outer 6.″5 pair HWE 81, known since 1876, has an estimated period of 10 kyr. Nordström et al. (2004) detected RV variability of the component A, later found to be a double-lined binary by Desidera et al. (2006). The orbital period is 21 days and the eccentricity $e = 0.766$ is unusually high for such a short period (Figure 10). The wide and shallow CCF dips imply fast axial rotation. For this reason, the RVs are not measured very accurately and the residuals to the orbit are large, 0.2 and 0.6 km s^{-1}. By comparing the estimated masses of Aa and Ab, 1.15 and 1.03 $\mathcal{M}_\odot$ respectively, with $M \sin^3 i$, I estimate the orbital inclination of 74°.

The visual component B also has a fast axial rotation of $V \sin i \sim 40$ km s^{-1}, degrading the accuracy of its RV

Table 5
Radial Velocities and Residuals (Fragment)

HIP/HD	System	Date (JD +24,00,000)	V_1	σ_1 (km s^{-1})	$(O-C)_1$	V_2	σ_2 (km s^{-1})	$(O-C)_2$
19639	Aa,Ab	57985.8910	68.74	0.30	0.16	−6.37	0.60	−0.42
19639	Aa,Ab	57986.8980	15.11	0.30	0.18	59.76	0.60	−1.15
19639	Aa,Ab	58052.6260	31.22	10.00	2.23	...	...	...
19639	Aa,Ab	58053.6080	22.97	0.50	1.26	54.35	1.00	1.89

(This table is available in its entirety in machine-readable form.)

Table 6
Radial Velocities of Other Components

HIP/HD	Comp.	Date (JD +24,00,000)	RV (km s^{-1})
19646	B	57985.8932	36.005
19646	B	58193.5386	35.944
105080	A	58193.7546	50.182
105080	A	58194.6308	50.198
105080	A	58195.6489	50.179
60845	BC	57985.4627	42.462
60845	BC	58193.7521	42.524
60845	BC	58194.6447	42.514
60845	BC	58195.6586	42.523
60845	BC	58177.7617	42.513
60845	BC	58232.5972	42.540
60845	BC	58242.5361	42.513
75663	A	57986.4885	−50.737
75663	A	58177.8100	−56.446
75663	A	58193.8257	−57.181
75663	A	58195.8323	−57.305
76816	B	57986.4996	−50.912
76816	B	58193.8413	−50.916
76816	B	58194.8267	−50.921
76816	B	58195.8509	−50.912
78163	B	57986.5130	6.116
78163	B	58194.8533	7.152
78163	B	58195.7872	7.082
78416	B	57986.5221	0.752
78416	B	58193.8595	1.568
78416	B	58194.8446	1.816
78416	B	58195.7774	1.581
80448	B	58193.8678	7.509
80448	B	58195.8008	7.752
80448	B	58194.8621	7.679
80448	B	58228.8113	7.515
80448	B	58233.8463	7.353
80448	B	58246.6693	8.395
80448	B	58248.8529	8.176
80448	B	58256.7395	7.532
80448	B	58257.8020	7.916
84789	B	57986.5346	6.669
84789	B	58195.8671	5.260

(This table is available in machine-readable form.)

measurement. The RVs of B measured with CHIRON, by *Gaia*, and by Desidera et al. (2006), 1.4, −0.7, and 0.5 km s^{-1}, respectively, are reasonably close to the center-of-mass RV of A, 1.7 km s^{-1}. Therefore, B is likely a single star. All three stars Aa, Ab, and B have comparable masses and similar colors. The component A, being a close pair, is located on the CMD just above B, as expected.

The RVs of Aa and Ab measured by Desidera et al. (2006), 58.9 and −1.8 km s^{-1}, correspond to the center-of-mass velocity of 30.2 km s^{-1} and do not fit the present orbit with $\gamma = 1.7$ km s^{-1}. This discrepancy suggests that Aa,Ab is orbited by another close companion. Further monitoring is needed, however, to prove this hypothesis.

According to Rizzuto et al. (2011), this system belongs to the Sco OB2 association with a probability of 74%. Fast axial rotation and the presence of lithium indicate a young age.

3.9. HIP 80448 (2+2 Quadruple)

This young multiple system is located within 50 pc from the Sun. It contains four components in a small volume. The outer pair A,B (COO 197) has an uncertain visual orbit with a millenium-long period (Argyle et al. 2015). Its secondary component was resolved in 2004 into a 0.″13 pair CVN 27 Ba,Bb by Chauvin et al. (2010), using adaptive optics. Independently, a subsystem TOK 50 Aa,Ab with similar separation was discovered in 2009 by Tokovinin et al. (2010) using speckle interferometry. In fact, the same subsystem Ba,Bb was wrongly attributed to the primary component; its published measures at SOAR with angle inverted by 180° match the preliminary orbit with $P_{\rm Ba,Bb} = 20$ years. The pair TOK 50 Aa,Ab does not exist. The component Bb is fainter than Ba by 3.5 mag in the V band and by 1.1 mag in the K band; its lines are not detected in the combined spectrum of all stars.

Figure 11 shows the positions of resolved components on the sky and the fitted orbits. Considering that the outer orbit is not constrained by the data, I fixed its period to $P_{\rm A,B} = 1950$ years and its axis to $a_{\rm A,B} = 4.''64$ to adjust the dynamical mass sum to its estimated value, 3.5 $\mathcal{M}_\odot$. The orbit of Ba,Bb with $P_{\rm Ba,Bb} = 20$ years yields the mass sum of 1.8 $\mathcal{M}_\odot$, close to the estimated one. The "wobble" in the positions of A,Ba caused by the subsystem is clearly seen. Its relative amplitude $f = 0.40$ corresponds to the mass ratio $q_{\rm Ba,Bb} = f/(1-f) = 0.67$ that agrees with the magnitude difference.

The spectrum of the main component A (in fact, blended light of Aa, Ab, and Ba) shows stationary lines of Ba and double lines of Aa and Ab in rapid motion; the subsystem Aa,Ab was discovered with CHIRON (Tokovinin 2015). It is found here that the orbital period is $P_{\rm Aa,Ab} = 2.3$ days and the orbit is circular (Figure 12). The mass ratio $q_{\rm Aa,Ab} = 0.67$ is similar to the mass ratio $q_{\rm Ba,Bb}$, while the ratio of dip areas corresponds to $\Delta V_{\rm Aa,Ab} = 1.9$ mag. Comparison of estimated and spectroscopic mass sums leads to the orbital inclination $i_{\rm Aa,Ab} = 66°$ or $i_{\rm Aa,Ab} = 114°$. It is not dissimilar to the inclination of the other inner pair, $i_{\rm Ba,Bb} = 109°$, but it is difficult to believe that these two subsystems have coplanar orbits, given the huge difference of their periods.

Table 7
Position Measurements and Residuals (Fragment)

HIP/HD	System	Date (year)	θ (°)	ρ (″)	σ_ρ (″)	$(O-C)_\theta$ (°)	$(O-C)_\rho$ (″)	Ref.[a]
60845	B,C	1939.4600	357.8	0.3500	0.1500	4.2	0.1351	M
60845	B,C	1956.3800	184.1	0.3100	0.0500	8.8	0.0956	M
60845	B,C	2018.1639	92.6	0.1769	0.0050	1.9	0.0070	S
60845	A,BC	1880.3800	270.5	2.4300	0.2500	2.2	0.3463	M
60845	A,BC	1991.2500	201.1	2.0510	0.0100	−1.2	−0.0042	H
60845	A,B	2018.1639	187.1	2.0965	0.0050	0.2	−0.0018	S

Note.
[a] H: *Hipparcos*; S: speckle interferometry at SOAR; s: speckle interferometry at other telescopes; M: visual micrometer measures; G: *Gaia* DR2.
(This table is available in its entirety in machine-readable form.)

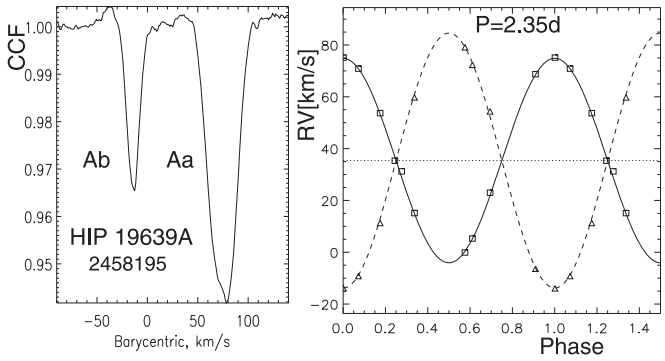

Figure 1. CCF (left) and RV curve (right) of HIP 19639 Aa,Ab.

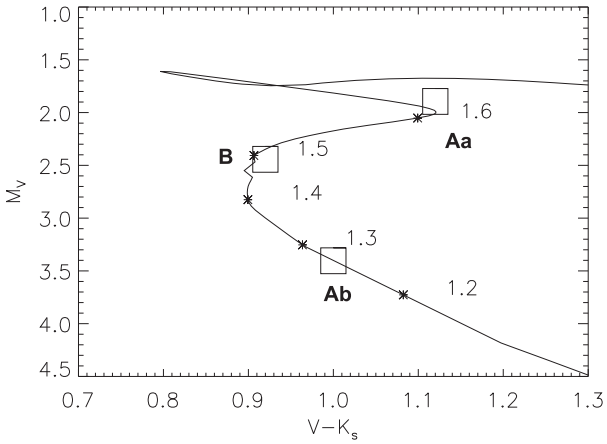

Figure 2. Location of three components of the HIP 19639 system on the color–magnitude diagram (squares). The full line is a 2 Gyr isochrone for solar metallicity (Dotter et al. 2008), where asterisks and numbers mark masses.

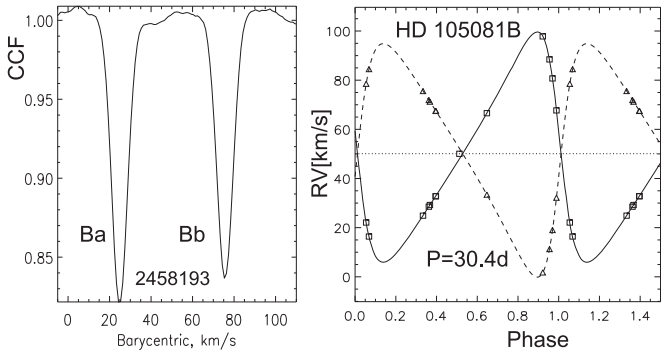

Figure 3. CCF (left) and RV curve (right) of HD 105081 Ba,Bb.

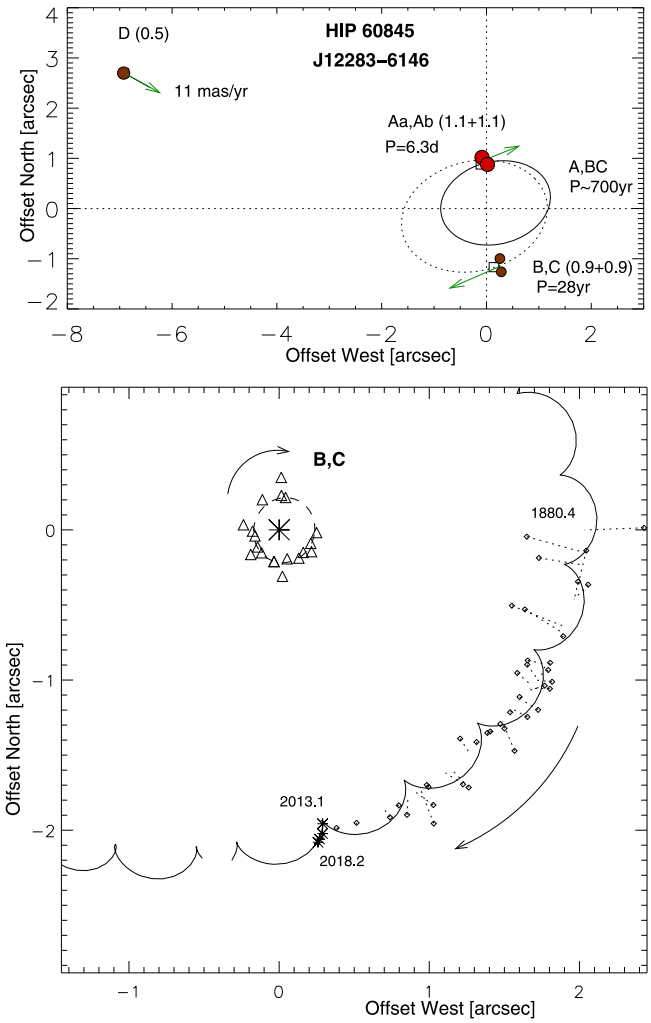

Figure 4. Quintuple system HIP 60845 (WDS J12283−6146). The positions of three components A, BC, and D on the sky and their motions are illustrated in the upper panel. Periods and masses are indicated. The lower panel shows the observed motion of the subsystems A,BC and B,C and their orbits. In this plot, the coordinate origin coincides with the main star A, the wavy line shows the motion of the component B around A according to the orbit. Small crosses depict measurements of A,BC where the pair BC was unresolved, asterisks depict the resolved measurents of A,B. The orbit of B,C is plotted on the same scale around the coordinate origin by the dashed line and triangles.

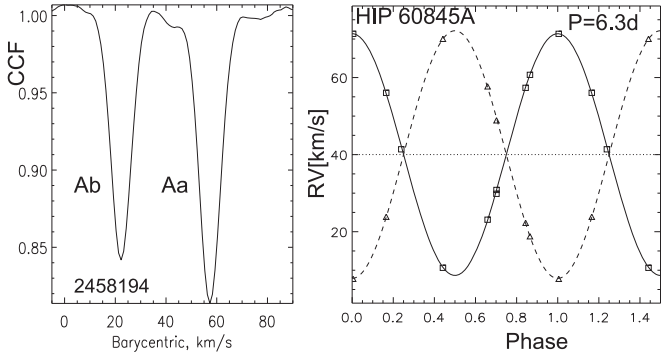

Figure 5. CCF (left) and RV curve (right) of HIP 60845 Aa,Ab.

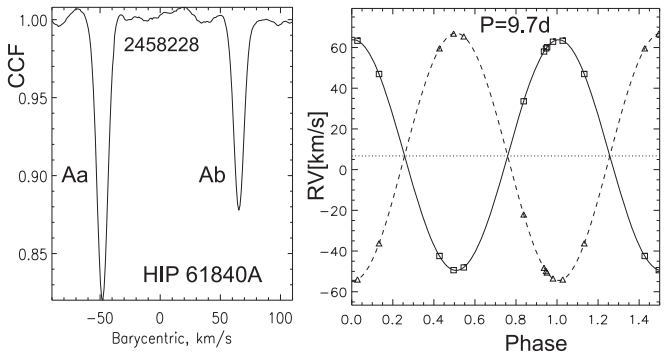

Figure 6. CCF (left) and RV curve (right) of HIP 61840 Aa,Ab.

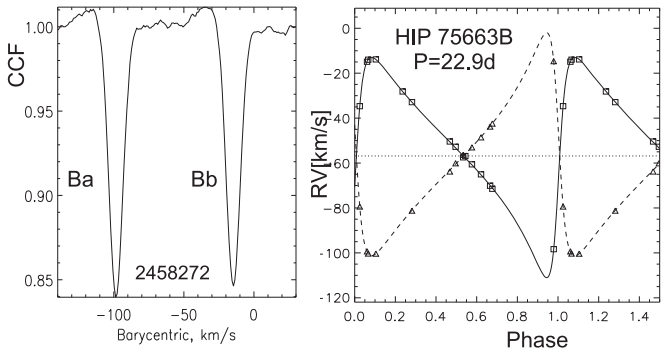

Figure 7. CCF (left) and RV curve (right) of HIP 75663 Ba,Bb.

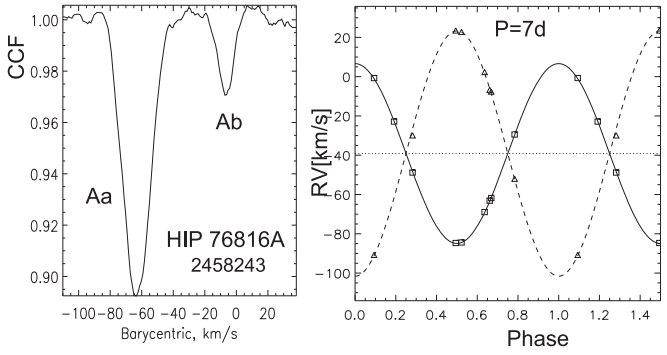

Figure 8. CCF (left) and RV curve (right) of HIP 76816 Aa,Ab.

The components Aa and Ab rotate synchronously with the orbit. The projected rotation of Ba, $V \sin i = 14.3\,\mathrm{km\,s^{-1}}$, is relatively fast, supporting the thesis that this system is young. The presence of lithium also suggests youth. The four components are located in the CMD at about 0.7 mag above the main sequence.

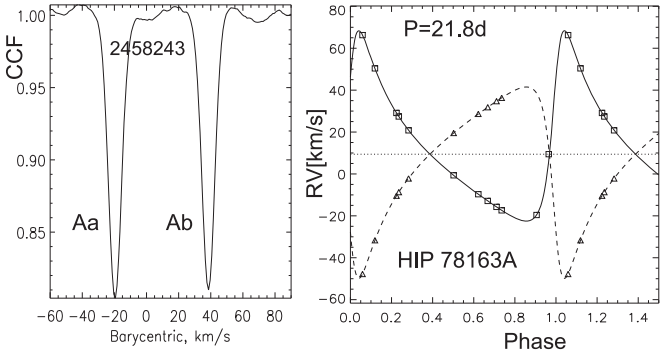

Figure 9. CCF (left) and RV curve (right) of HIP 78163 Aa,Ab.

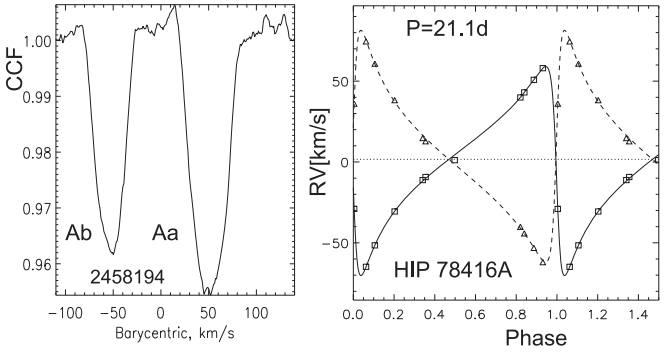

Figure 10. CCF (left) and RV curve (right) of HIP 78416 Aa,Ab.

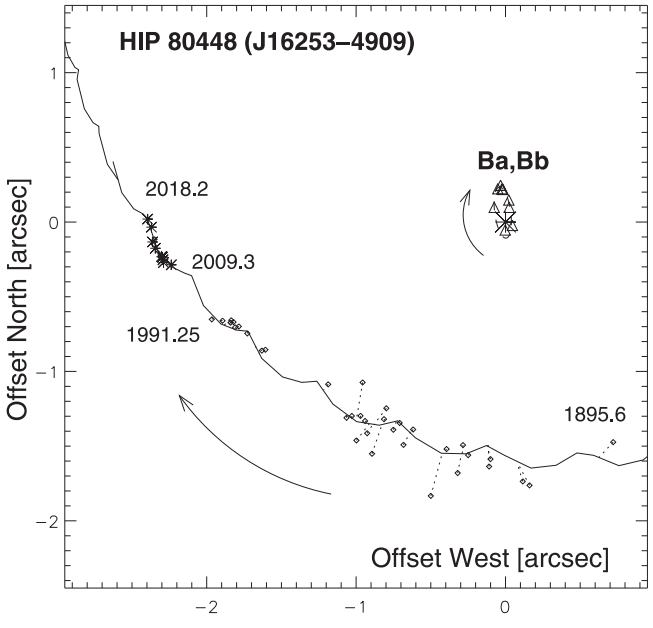

Figure 11. Visual orbits of HIP 80448 A,B and Ba,Bb (WDS J16253−4909, COO 197 and CVN 27).

The pair Ba,Bb is presently near the periastron of its 20 year orbit. I measured the RV(Ba) from 7.51 to 8.18 km s^{-1}, quite different from the center-of-mass velocity of A, $-2.08\,\mathrm{km\,s^{-1}}$. This positive difference and the positive trend actually match the orbit of Ba,Bb; I predict that RV(Ba) will soon start to

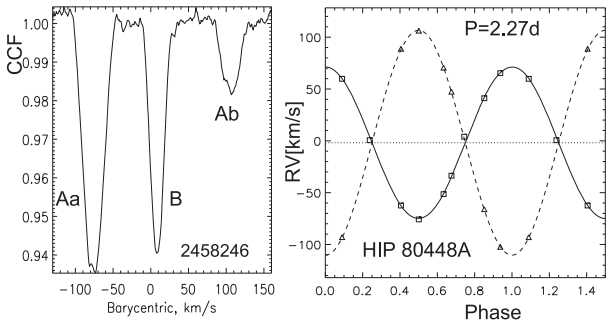

Figure 12. CCF (left) and RV curve (right) of HIP 80448 Aa,Ab.

decrease. The orbits of A,B and Ba,Bb are not coplanar, although both are retrograde.

3.10. HIP 84789 (Triple)

This 5.″6 visual binary STF 2148, discovered in 1832 by W. Struve, has an estimated period of 17 kyr. Double lines in its primary component A were noted by Nordström et al. (2004). The orbital period of the subsystem Aa,Ab determined here is $P_{\rm Aa,Ab} = 2.3$ days; it is a twin pair with $q_{\rm Aa,Ab} = 0.988$ (Figure 13). The deeper CCF dip belongs to the less massive component Ab; the more massive star Aa rotates a little faster and has a dip area 3% larger than Ab, as well as the smaller RV amplitude. The RVs of both components are measured with large errors owing to the wide and low-contrast CCF dips; the residuals to the orbits are also large. An attempt to fit the orbit with nonzero eccentricity does not result in smaller residuals, hence the orbit is circular.

The estimated masses of Aa and Ab are 1.30 $\mathcal{M}_\odot$ each, leading to the orbital inclination of $i_{\rm Aa,Ab} = 45°$. Assuming the radii of 1.3 $R_\odot$, the synchronous rotation velocity is $V \sin i = 20.2\,{\rm km\,s^{-1}}$. The width of the correlation dips matches this estimate and suggests that Aa rotates slightly faster and Ab slightly slower than synchronous.

The two components A and B are located on the CMD above each other (they have the same color) because A contains two equal stars; the mass of B is very similar to the masses of Aa and Ab, 1.3 solar. The component B is single, as inferred from the equality of its RV to the center-of-mass velocity of A. However, it rotates much faster, at $V \sin i \sim 49\,{\rm km\,s^{-1}}$. Very likely, the rotation of Aa and Ab has been slowed down by tidal synchronization with the orbit.

4. Summary

Probably by accident, the periods of nine spectroscopic systems within hierarchical multiples are equally divided between three distinct groups: (i) circular orbits with $P \approx 2.3$ days, (ii) intermediate periods between 6 and 9 days, circular or nearly circular, and (iii) eccentric orbits with periods from 21 to 30 days. Figure 14 places these orbits on the period–eccentricity plot. The plus signs are 467 spectroscopic binaries with primary masses from 0.5 to 1.5 $\mathcal{M}_\odot$ from the MSC (Tokovinin 2018a). When the eccentric orbits of the group (iii) are tidally circularized, their periods will match those of group (ii), suggesting that these subsystems could be formed by a common mechanism, such as Kozai–Lidov cycles with dynamical tides (Moe & Kratter 2018). The periods of group (i) are substantially shorter, so their formation history could be different.

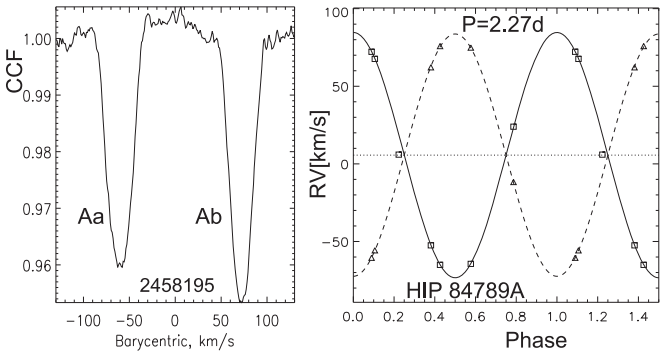

Figure 13. CCF (left) and RV curve (right) of HIP 84789 Aa,Ab. Note that the secondary component Ab has a dip with larger amplitude.

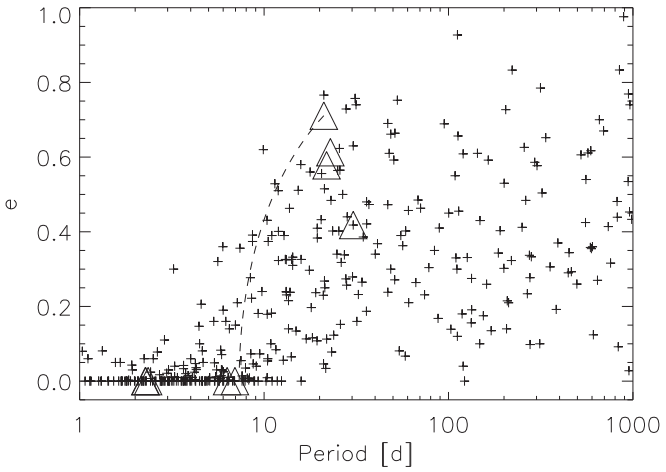

Figure 14. Eccentricity vs. period for members of hierarchical systems studied here (large triangles) and for 467 spectroscopic binaries from the MSC with primary masses from 0.5 to 1.5 solar (crosses). The dashed line shows the locus of HIP 78416 Aa,Ab for evolution with constant angular momentum, $P(1-e^2)^{3/2} = {\rm const}$.

Six out of the 10 double-lined binaries studied here are twins with mass ratio $q > 0.95$, while the lowest measured mass ratio is 0.67. If the mass ratios were uniformly distributed in the interval (0.7, 1.0), where double lines are detectable, the fraction of twins would be only 0.15, whereas in fact it is 0.6. It is established that twins correspond to a well-defined peak in the mass ratio distribution of solar-type spectroscopic binaries (Tokovinin 2000). They are believed to be formed when a low-mass binary accretes a major part of its mass. The mass influx also creates conditions for formation of additional components, building stellar hierarchies "from inside out." Thus, twins are naturally produced as inner components of multiple systems in the process of mass assembly.

The goal of this study was to determine unknown periods of spectroscopic subsystems in several multiple stars. Although this goal is reached, I discovered RV variability of other visual components (HIP 75663A, 76816B, and 78163B), converting these triples into 2 + 2 quadruples. The periods of new subsystems, presumably long, remain unknown so far.

I thank the operator of the 1.5 m telescope R. Hinohosa for executing observations of this program and L. Paredes for scheduling and pipeline processing. Reopening of CHIRON in 2017 was largely due to the enthusiasm and energy of T. Henry.

This work used the SIMBAD service operated by Centre des Données Stellaires (Strasbourg, France), bibliographic references from the Astrophysics Data System maintained by SAO/NASA, and the Washington Double Star Catalog maintained at USNO.

This work has made use of data from the European Space Agency (ESA) mission *Gaia* (https://www.cosmos.esa.int/gaia), processed by the *Gaia* Data Processing and Analysis Consortium (DPAC, https://www.cosmos.esa.int/web/gaia/dpac/consortium). Funding for the DPAC has been provided by national institutions, in particular, the institutions participating in the *Gaia* Multilateral Agreement.

Facilities: CTIO:1.5 m, SOAR.

ORCID iDs

Andrei Tokovinin https://orcid.org/0000-0002-2084-0782

References

Argyle, R. W., Alzner, A., & van Leeuwen, F. 2015, AN, 336, 378
Chauvin, G., Lagrange, A.-M., Bonavita, M., et al. 2010, A&A, 509, 52
Desidera, S., Gratton, R. G., Lucatello, S., et al. 2006, A&A, 454, 553
Dotter, A., Chaboyer, B., Jevremović, D., et al. 2008, ApJS, 178, 89
Gaia Collaboration, Prusti, T., de Bruijne, J. H. J., et al. 2016, A&A, 595A, 1
Isaacson, H., & Fischer, D. 2010, ApJ, 725, 875
Mason, B. D., Wycoff, G. L., Hartkopf, W. I., Douglass, G. G., & Worley, C. E. 2001, AJ, 122, 3466, (WDS)
Moe, M., & Kratter, K. M. 2018, ApJ, 854, 44
Nordström, B., Mayor, M., Andersen, J., et al. 2004, A&A, 418, 989
Rizzuto, A. C., Ireland, M. J., & Robertson, J. G. 2011, MNRAS, 416, 3108
Seymour, D., Mason, B. D., Hartkopf, W. I., & Wycoff, G. L. 2002, AJ, 123, 1023
Tokovinin, A. 2014, AJ, 147, 86
Tokovinin, A. 2015, AJ, 150, 177
Tokovinin, A. 2016a, AJ, 152, 11, (Paper I)
Tokovinin, A. 2016b, AJ, 152, 10, (Paper II)
Tokovinin, A. 2016c, ORBIT: IDL Software for Visual, Spectroscopic, and Combined Orbits, Zenodo, doi:10.5281/zenodo.61119
Tokovinin, A. 2017, ORBIT3—Orbits of Triple Stars, Zenodo, doi:10.5281/zenodo.321854
Tokovinin, A. 2018a, ApJS, 235, 6, (MSC)
Tokovinin, A. 2018b, AJ, 156, 48, (Paper III)
Tokovinin, A., Fischer, D. A., Bonati, M., et al. 2013, PASP, 125, 1336
Tokovinin, A., & Latham, D. W. 2017, ApJ, 838, 54
Tokovinin, A., Mason, B. D., & Hartkopf, W. I. 2010, AJ, 139, 743
Tokovinin, A., Mason, B. D., Hartkopf, W. I., et al. 2018, AJ, 155, 235
Tokovinin, A. A. 2000, A&A, 360, 997
Udry, S., Mayor, M., & Queloz, D. 1998, in ASP Conf. Ser. 185, Precise Stellar Radial Velocities, ed. J. B. Hearnshaw & C. D. Scarfe (San Francisco, CA: ASP), 367
Wichman, R., Schmitt, J. H. M. M., & Hubrig, S. 2003, A&A, 400, 293